TS-ACL: A Time Series Analytic Continual Learning Framework for Privacy-Preserving and Class-Incremental Pattern Recognition

Kejia Fan[1]*, Jiaxu Li[1]*, Songning Lai[2]*, Linpu Lv[3], Jianheng Tang[4]†,
Anfeng Liu[1], Houbing Herbert Song[5], Yutao Yue[2], Huiping Zhuang[6]†
[1]Central South University, [2]The Hong Kong University of Science and Technology (Guangzhou),
[3]Zhengzhou University, [4]Peking University, [5]University of Maryland, Baltimore County,
[6]South China University of Technology

Abstract

*Class-incremental pattern recognition in time series is a significant problem, which aims to learn from continually arriving streaming data examples with incremental classes. A primary challenge in this problem is catastrophic forgetting, where the incorporation of new data samples causes the models to forget previously learned information. While the replay-based methods achieve promising results by storing historical data to address catastrophic forgetting, they come with the invasion of data privacy. On the other hand, the exemplar-free methods preserve privacy but suffer from significantly decreased accuracy. To address these challenges, we proposed **TS-ACL**, a novel **T**ime **S**eries **A**nalytic **C**ontinual **L**earning framework for privacy-preserving and class-incremental pattern recognition. Identifying gradient descent as the root of catastrophic forgetting, TS-ACL transforms each update of the model into a gradient-free analytical learning process with a closed-form solution. By leveraging a pre-trained frozen encoder for embedding extraction, TS-ACL only needs to recursively update an analytic classifier in a lightweight manner. This way, TS-ACL simultaneously achieves non-forgetting, privacy preservation, and lightweight consumption, making it widely suitable for various applications, particularly in edge computing scenarios. Extensive experiments on five benchmark datasets confirm the superior and robust performance of TS-ACL compared to existing advanced methods. Code is available at https://github.com/asdasdczxczq/TS-ACL.*

1. Introduction

With significant research attention in recent years, pattern recognition in time series plays a critical role in various
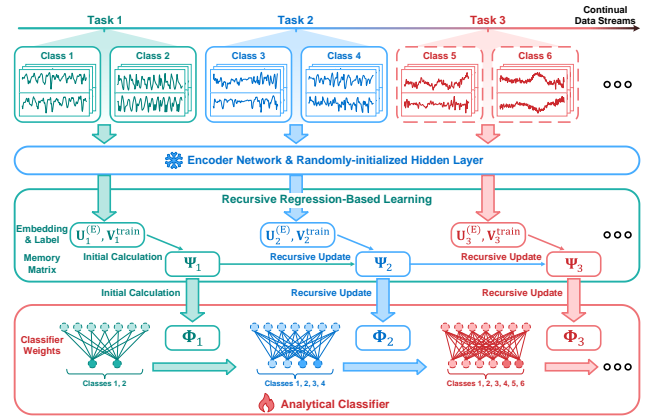

Figure 1. Overview of class-incremental pattern recognition in time series, in which our TS-ACL can simultaneously achieve non-forgetting, privacy preservation, and lightweight consumption.

applications, such as healthcare diagnostics [32], industrial production [36], and urban computing [13]. Deep Learning (DL) approaches have gained widespread popularity due to their superior performance, and they typically rely on offline, static datasets that assume data to be independently and identically distributed (i.i.d.) [10].

Unfortunately, as shown in Figure 1, real-world scenarios often involve continual data streams from sensors, resulting in an ever-growing volume of time series data with incremental classes, where the i.i.d. assumption no longer holds [23]. Additionally, as new data with previously unseen classes may emerge over time, the dataset becomes increasingly complex [23]. This dynamic environment requires the DL models to continually adapt and learn from new data samples. Unfortunately, this process is often hindered by the well-known problem of "catastrophic forgetting", in which the models forget previously learned knowledge when exposed to new data samples [5, 33].

To mitigate catastrophic forgetting, numerous Class-

---

*The first three authors contributed equally to this work.

†Corresponding authors: tangentheng@gmail.com, hpzhuang@scut.edu.cn.

Incremental Learning (CIL) methods have been proposed. These methods can be broadly categorized into two types: the *replay-based* methods [11, 25, 26] and the *exemplar-free* methods [1, 12, 23]. The *replay-based* methods store historical samples or use generative models to produce synthetic samples, called the exemplar, to enable the model to retain previously learned knowledge [25, 26, 28]. While these *replay-based* methods can achieve impressive performance, they inherently raise significant concerns about privacy due to the need to store historical data [39]. More importantly, in many practical applications, particularly edge computing scenarios, the limited storage and computational resources usually render such methods impractical [17]. On the other hand, the *exemplar-free* methods typically aim to protect learned knowledge by modifying the loss function or optimizing the learning process without exemplar [12, 33]. Although these methods avoid privacy issues, they still suffer from significantly decreased accuracy with suboptimal performance, limiting their practical utility [40].

Furthermore, a more fundamental and general limitation within current CIL methods, whether the *replay-based* or the *exemplar-free*, lies in their reliance on gradient-based backpropagation techniques. Since gradients computed from new data can conflict with or even contradict those derived from historical data, current CIL methods fail to fully address the problem of catastrophic forgetting. As a result, updates based on conflicting gradients inevitably lead to the erasure of previously acquired knowledge [5].

To address these challenges, we introduce a novel **T**ime **S**eries **A**nalytic **C**ontinual **L**earning framework, named **TS-ACL**, for privacy-preserving and class-incremental pattern recognition, as shown in Figure 1. Identifying gradient descent as the root of catastrophic forgetting, TS-ACL transforms each update of the model into a gradient-free analytical learning process with a closed-form solution, Thus, TS-ACL completely removes the need for gradient-based updates and fundamentally solves the issue of catastrophic forgetting. By leveraging a pre-trained frozen encoder for embedding extraction, TS-ACL only needs to recursively update an analytic classifier for each task in a lightweight manner. This way, TS-ACL simultaneously achieves non-forgetting, privacy preservation, and lightweight consumption. The key contributions of this work are as follows:

1. We propose a novel TS-ACL framework for privacy-preserving and class-incremental pattern recognition. By introducing analytic learning to replace gradient descent, TS-ACL achieves insightful non-forgetting, thereby fundamentally solving the issue of catastrophic forgetting.
2. With the least squares method for each update, TS-ACL achieves lightweight consumption in both computation and storage, making it highly suitable for various applications, especially in edge computing scenarios.
3. Through theoretical analysis, we prove that TS-ACL's

performance on incremental tasks is fully equivalent to joint training on all tasks, ensuring its remarkable property of "non-forgetting".
4. Comprehensive experiments validate the state-of-the-art performance of TS-ACL. Our TS-ACL, as an *exemplar-free* method, not only far surpasses other *exemplar-free* baselines, but also demonstrates amazing competitiveness even compared to the *replay-based* ones.

2. Related Work

2.1. Pattern Recognition in Time Series

Pattern recognition in time series aims to assign categorical labels to time series data based on its patterns or characteristics, playing an increasingly important role in numerous domains [19, 32, 36]. In the early stages of research, the focus was primarily on non-DL methods, which mainly included distance-based methods [14, 29] and ensembling methods [15, 18]. The distance-based methods rely on various time series distance measurement techniques, with the Dynamic Time Warping as a representative example [9], using 1-nearest neighbor classifiers. The ensembling methods integrate multiple individual 1-nearest neighbor classifiers with different distance metrics to achieve improved performance [15, 19]. These non-DL methods typically incur significant computational overhead and struggle with scalability when applied to large-scale datasets [8, 19].

Recently, DL-based methods have been extensively studied and have achieved encouraging performance [8, 23, 31]. These methods are typically trained on offline, static, and i.i.d. datasets, with little consideration given to scenarios involving continual data perception in real-world environments [23]. In practice, new time series data samples are continually collected over time, necessitating incremental model updates [23, 33]. Unfortunately, classical DL-based methods inevitably face the problem of "catastrophic forgetting", where the models forget previously learned knowledge when exposed to new data samples [5, 33].

2.2. Class-incremental Learning

To alleviate the problem of catastrophic forgetting, numerous studies on CIL [11, 12, 33] have emerged and can be broadly categorized into two main types: the *replay-based* methods [25, 25, 26] and the *examplar-free* methods [1, 12, 23]. The *replay-based* methods store a subset of historical samples, called the exemplar, and replay them during incremental training to alleviate the problem of catastrophic forgetting [26, 28]. Meanwhile, the *examplar-free* methods attempt to preserve prior knowledge by incorporating additional terms into the loss function or by explicitly designing and manipulating the optimization process [1, 23].

In practice, the *replay-based* methods typically achieve better performance thanks to the exemplar, but they inher-
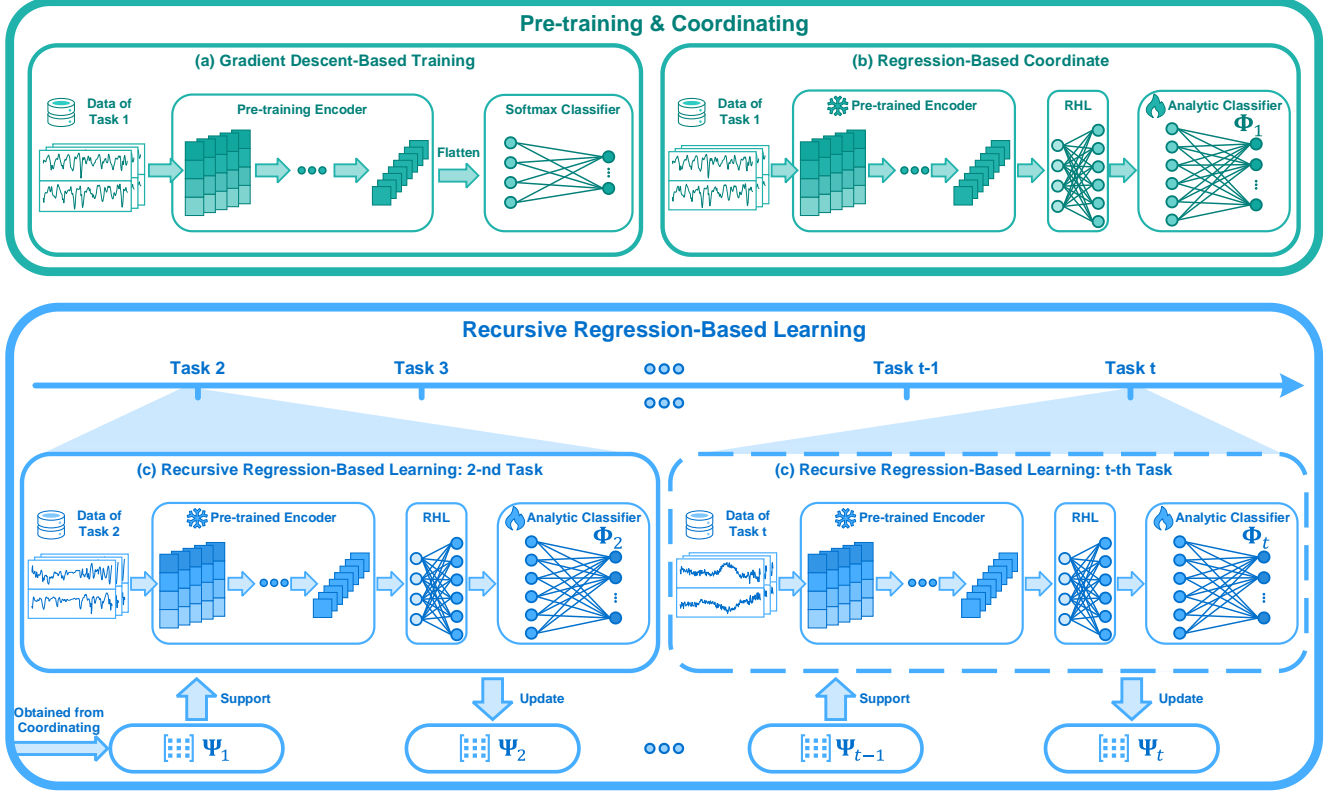
Figure 2. Overview of the proposed TS-ACL framework. In (a), a pre-trained encoder is first obtained on Task 1 through Gradient Descent-Based Training. Next, as shown in (b), a Regression-Based Coordinate module with an RHL is introduced before the classification head to enhance the embedding dimension, resulting in $\mathbf{\Psi_1}$ from Task 1 data. Finally, in (c), a Recursive Regression-Based Learning process is applied to achieve non-forgetting across tasks.

ently raise significant concerns about privacy [39]. In many practical applications, particularly edge computing scenarios, the limited storage and computational resources usually render such methods impractical [17]. Meanwhile, although the *exemplar-free* methods can avoid privacy issues, they typically suffer from significantly suboptimal performance [33, 40]. More critically, both these methods depend on gradient-based updating techniques, which fundamentally do not solve the problem of catastrophic forgetting [5].

2.3. Analytic Learning

Analytic learning, as a distinct technical pathway from gradient-based methods, has attracted considerable research attention in recent years [6, 30]. Specifically, the main idea of analytic learning is to directly compute the parameters of neural networks using mathematical methods such as least squares, thereby eliminating the need for gradients [30, 39]. For example, the radial basis network [20] use least-squares estimation to train parameters after the kernel transformation in the first layer. The multilayer analytic learning [34] transforms nonlinear network learning into segments, and efficiently solves this problem using least-squares tech-

niques in a single-epoch training process. Recently, several analytic learning-based CIL methods [38–40] have been proposed, which utilize least-squares techniques to directly compute the closed-form solutions for neural network in CIL scenario. We highlight that the gradient-free nature of analytic learning offers a foundational solution to catastrophic forgetting. Building on this, we propose TS-ACL, an analytic learning approach specifically crafted for class-incremental pattern recognition in time series, ensuring absolute knowledge retention without forgetting.

3. Method

3.1. Preliminaries

Let the model be continually trained for T tasks, where the training data for each task comes from different classes. Let $\mathcal{D}_t^{\text{train}} \sim \{\mathbf{U}_t^{\text{train}}, \mathbf{V}_t^{\text{train}}\}$ and $\mathcal{D}_t^{\text{test}} \sim \{\mathbf{U}_t^{\text{test}}, \mathbf{V}_t^{\text{test}}\}$ denote the training and testing datasets at task t ($t = 1, \ldots, T$). Specifically, $\mathbf{U}_t \in \mathbb{R}^{N_t \times c \times l}$ (e.g., N_t time series with a shape of $c \times l$) and $\mathbf{V}_t^{\text{train}} \in \mathbb{R}^{N_t \times d_{y_t}}$ (with task t containing d_{y_t} classes) represent the stacked input and label tensors.

In the CIL scenario, the classes learned across different

tasks are independent and non-overlapping [24, 33]. For each task t, the network learns from $\mathcal{D}_t^{\text{train}}$ and $\mathcal{D}_t^{\text{test}}$, where the classes differ from those in previous tasks. In task t, the data labels $\mathbf{V}_t^{\text{train}}$ and $\mathbf{V}_t^{\text{test}}$ belong to a task-specific class set $\mathcal{C}_t$, disjoint from other sets $\mathcal{C}_{t'}$ (for $t' \neq t$). Thus, data from different tasks exhibit distinct class distributions. For each task t, the objective is to use previous parameters Θ_{t-1} and $\mathcal{D}_t^{\text{train}}$ to update the model to Θ_t, ensuring both *stability* (retaining past knowledge) and *plasticity* (learning new knowledge).

Our proposed TS-ACL, comprising Gradient Descent-Based Training, Regression-Based Coordinate, and Recursive Regression-Based Learning as shown in Figure 2, achieves both stability and plasticity. TS-ACL ensures absolute retention of past knowledge, guaranteeing incremental learning is equivalent to joint training, where all tasks are learned simultaneously. This provides rigorous assurance of high accuracy across past and current tasks.

3.2. Gradient Descent-Based Training

First, we use gradient descent to train a regular classification network on the basic training task, which usually includes multiple training epochs. Theoretically, it can be composed of any commonly used network structure with a softmax classifier. After training, the output V of the network can be expressed as:

$$\mathbf{V} = f_{\text{softmax}}(f_{\text{flat}}(f_{\text{encoder}}(\mathbf{U}, \Theta_{\text{encoder}}))\boldsymbol{\Phi}), \qquad (1)$$

where Θ_{encoder} and $\boldsymbol{\Phi}$ are the parameters representing the encoder network and the classifier, $f_{\text{encoder}}(\mathbf{U}, \Theta_{\text{encoder}})$ represents the encoder output, f_{softmax} and f_{flat} are the softmax function and the flattening operator. After training, we save and freeze the encoder weights and treat the encoder as a embedding exactor.

3.3. Regression-Based Coordinate

Upon completing Gradient Descent-Based Training, we proceed with the Regression-Based Coordinate step using the analytical classifier replacing the softmax classifier. This process is carried out by the analytic classifier as the core mechanism, and briefly consists of three sub-steps:

The first sub-step involves extracting the embedding matrix (denoted as $\mathbf{U}_1^{(\text{encoder})}$) by passing the input tensor $\mathbf{U}_1^{\text{train}}$ through the trained encoder network, followed by a flattening operation, i.e.,

$$\mathbf{U}_1^{(\text{encoder})} = f_{\text{flat}}(f_{\text{encoder}}(\mathbf{U}_1^{\text{train}}, \Theta_{\text{encoder}})), \qquad (2)$$

where $\mathbf{U}_1^{(\text{encoder})} \in \mathbb{R}^{N_1 \times d_{\text{encoder}}}$. Next, instead of directly mapping the embeddings to the classification output via a single classifier layer, we add a Randomly-initialized Hidden Layer (RHL). Specifically, the embedding $\mathbf{U}_1^{(\text{encoder})}$ is

expanded into $\mathbf{U}_1^{(\text{E})}$ as follows:

$$\mathbf{U}_1^{(\text{E})} = f_{\text{act}}(\mathbf{U}_1^{(\text{encoder})}\boldsymbol{\Phi}^{\text{E}}), \qquad (3)$$

where $\mathbf{U}_1^{(\text{E})} \in \mathbb{R}^{N_1 \times d_{\text{E}}}$, with d_{E} representing the embedding expansion size (generally $d_{\text{encoder}} < d_{\text{E}}$). Here, f_{act} refers to the activation function, and $\boldsymbol{\Phi}^{\text{E}}$ is the matrix used to expand the encoder-extracted embeddings. The matrix $\boldsymbol{\Phi}^{\text{E}}$ is initialized by sampling its elements from a normal distribution.

Why need RHL? The necessity of the RHL layer lies in the need for a larger parameter space for analytical learning. By projecting the original embeddings into a higher-dimensional space, it enables the model to fully realize its potential. This projection allows the model to express more complex relationships within the data, which are difficult to capture in a lower-dimensional space.

Finally, the expanded embeddings $\mathbf{U}_1^{(\text{E})}$ are mapped to the label matrix $\mathbf{V}_1^{\text{train}}$ using a linear regression procedure, by solving the following optimization problem:

$$\arg\min_{\boldsymbol{\Phi}_1} \left\| \mathbf{V}_1^{\text{train}} - \mathbf{U}_1^{(\text{E})}\boldsymbol{\Phi}_1 \right\|_F^2 + \gamma \left\| \boldsymbol{\Phi}_1 \right\|_F^2, \qquad (4)$$

where γ is a regularization parameter. The solution to this problem is given by:

$$\widehat{\boldsymbol{\Phi}}_1 = \left(\mathbf{U}_1^{(\text{E})\top}\mathbf{U}_1^{(\text{E})} + \gamma\mathbf{I} \right)^{-1} \mathbf{U}_1^{(\text{E})\top}\mathbf{V}_1^{\text{train}}, \qquad (5)$$

where the notation $\top$ is the transposed operation and the notation $^{-1}$ represent the inverse operation.

3.4. Recursive Regression-Based Learning

After completing the Regression-Based Coordinate, we proceed with the CIL process using Recursive Regression-Based Learning in a recursive and analytical manner. To demonstrate this, without loss of generality, assume we are given $\mathcal{D}_1^{\text{train}}, \dots, \mathcal{D}_{t-1}^{\text{train}}$, and let

$$\mathbf{U}_{1:t-1}^{(\text{E})} \in \mathbb{R}^{N_{1:t-1} \times d_{\text{E}}}, \quad \mathbf{V}_{1:t-1} \in \mathbb{R}^{N_{1:t-1} \times \sum_{i=1}^{t-1} d_{y_i}} \quad (6)$$

represent the concatenated activation and label tensors, respectively, from task 1 to $t - 1$, i.e.,

$$\mathbf{U}_{1:t-1}^{(\text{E})} = \begin{bmatrix} \mathbf{U}_1^{(\text{E})} \\ \vdots \\ \mathbf{U}_{t-1}^{(\text{E})} \end{bmatrix}, \quad \mathbf{V}_{1:t-1} = \begin{bmatrix} \mathbf{V}_1^{\text{train}} & \cdots & 0 \\ \vdots & \ddots & \vdots \\ 0 & \cdots & \mathbf{V}_{t-1}^{\text{train}} \end{bmatrix}. \qquad (7)$$

Here, $N_{1:t-1}$ indicates the total number of data samples from task 1 to $t - 1$. The sparse structure of $\mathbf{V}_{1:t-1}$ arises because of the mutually exclusive classes across tasks. The learning problem can then be formulated as follows:

$$\arg\min_{\boldsymbol{\Phi}_{t-1}} \left\| \mathbf{V}_{1:t-1} - \mathbf{U}_{1:t-1}^{(\text{E})}\boldsymbol{\Phi}_{t-1} \right\|_F^2 + \gamma \left\| \boldsymbol{\Phi}_{t-1} \right\|_F^2, \quad (8)$$

according to 5, at task $t-1$, we have:

$$\hat{\boldsymbol{\Phi}}_{t-1} = \left(\mathbf{U}_{1:t-1}^{(E)\top}\mathbf{U}_{1:t-1} + \gamma\mathbf{I}\right)^{-1}\mathbf{U}_{1:t-1}^{(E)\top}\mathbf{V}_{1:t-1}, \quad (9)$$

where $\hat{\boldsymbol{\Phi}}_{t-1} \in \mathbb{R}^{d_E \times \sum_{i=1}^{t-1} d_{y_i}}$, with the column size expanding as t increases. Let

$$\boldsymbol{\Psi}_{t-1} = \left(\mathbf{U}_{1:t-1}^{(E)\top}\mathbf{U}_{1:t-1} + \gamma\mathbf{I}\right)^{-1} \quad (10)$$

denote the aggregated temporal inverse correlation matrix, which captures the correlation information from both current and past samples. Based on this, out goal is to compute $\hat{\boldsymbol{\Phi}}_t$ using only $\hat{\boldsymbol{\Phi}}_{t-1}$, $\boldsymbol{\Psi}_{t-1}$, and the current task's data $\mathbf{U}_t^{train}$, without involving historical samples such as $\mathbf{U}_{1:t-1}$. The process is formulated in the following theorem.

Theorem 1. *The $\boldsymbol{\Phi}$ weights, recursively obtained by*

$$\hat{\boldsymbol{\Phi}}_t = \left[\hat{\boldsymbol{\Phi}}_{t-1} - \boldsymbol{\Psi}_t\mathbf{U}_t^{(E)}\mathbf{U}_t^{(E)\top}\hat{\boldsymbol{\Phi}}_{t-1} \quad \boldsymbol{\Psi}_t\mathbf{U}_t^{(E)\top}\mathbf{V}_t^{train}\right] \tag{11}$$

are equivalent to those obtained from 9 for task t. The matrix $\boldsymbol{\Psi}_t$ can also be recursively updated by

$$\boldsymbol{\Psi}_t = \boldsymbol{\Psi}_{t-1} - \boldsymbol{\Psi}_{t-1}\mathbf{U}_t^{(E)}\left(\mathbf{I} + \mathbf{U}_t^{(E)\top}\boldsymbol{\Psi}_{t-1}\mathbf{U}_t^{(E)}\right)^{-1}\mathbf{U}_t^{(E)\top}\boldsymbol{\Psi}_{t-1}. \tag{12}$$

Proof. See the supplementary materials. □

As stated in Theorem 1, the proposed TS-ACL framework provides a recursive update for the $\boldsymbol{\Phi}$ weights without losing any historical information. First, the base model is trained on the initial dataset (e.g. to compute $\hat{\boldsymbol{\Phi}}_1$), and the CIL process continues using the recursive formulation to obtain $\hat{\boldsymbol{\Phi}}_t$ for $t > 1$.

Privacy-Preserving and High-Performance. TS-ACL safeguards privacy in two significant ways: first, by avoiding the use of historical data samples, and second, by ensuring impossible to use reverse engineering to obtain historical data samples from the $\boldsymbol{\Psi}$ matrix. As an exemplar-free method, TS-ACL differs from other exemplar-free approaches, which often exhibit considerable performance gaps compared to replay-based methods. In contrast, TS-ACL performs on par with or even surpasses replay-based methods, as shown in the following experiments. TS-ACL not only upholds privacy but also achieves high performance, and this dual benefit is particularly valuable in today's era of increased data privacy concerns.

4. Experiment

4.1. Setup

Datasets. Following [24] We continued previous research by selecting five balanced time series datasets, each containing samples with the same length and variables, which is shown in Table 1. See supplementary for more details.

Table 1. Time series dataset details which is sourced from [24].

Dataset	Shape ($C \times L$)	Train Size	Test Size	# Classes	# Exp Tasks
UCI-HAR [7]	9×128	7352	2947	6	3
UWave [16]	3×315	896	3582	8	4
DSA [2]	45×125	6840	2280	18	6
GRABMyo [22]	28×128	36120	12040	16	5
WISDM [35]	3×200	18184	6062	18	6

CIL Setting. We trained and evaluated on five datasets, each divided into n tasks with two distinct classes per task, and randomly shuffled class order before partitioning. To evaluate the robustness, we used different random seeds to conduct five independent experiments and report the average results with standard deviation.

Task Stream. Following [24], we divided tasks into a validation stream and an experiment stream. In the UCI-HAR [7] and UWave datasets [16], both the validation and experimental streams consist of 3 and 4 tasks, respectively. And other datasets include three tasks in the validation stream, with the experimental stream covering the remaining tasks, as summarized in Table 1. We initially perform a grid search on the validation stream to optimize hyperparameters, then use the selected parameters to conduct experiments on the experiment stream.

Comparison Baselines. Following [24], for *examplar-free* methods, we selected 3 classical baselines: *LwF* [12], *MAS* [1], and *DT²W* [23]. For *replay-based* methods, we chose 7 up-to-date baselines: *GR* [28], *ER* [26], *ICARL* [25], *DER* [3], *ASER* [27], *CLPOS* [10] and *FASTICARL* [11].

Evaluation Metrics. To quantitatively assess the performance of CIL methods, we utilize two widely adopted metrics: *Average accuracy* and *Forgetting*. *Average accuracy* is calculated by averaging the accuracy of all previously encountered tasks, including the current task after learning the current task t. It is defined as $\mathcal{A}_t = \frac{1}{t}\sum_{i=1}^{t}\mathcal{A}_{t,i}$, where $\mathcal{A}_{t,i}$ represents the accuracy on task i after learning task t. *Forgetting* is measured to capture how much performance degrades on previous tasks after learning a new task t. It is computed as $\mathcal{F}_t = \frac{1}{t-1}\sum_{i=1}^{t-1}\left(\max_{j\in\{1,\ldots,t-1\}}\mathcal{A}_{j,i} - \mathcal{A}_{t,i}\right)$. At task t, the forgetting on task i is defined as the maximum difference between the highest accuracy previously achieved on task i and the accuracy on task i after learning task t.

Selected encoder. We adopted the same 1D-CNN encoder network structure as in [24]. The network comprises four convolutional blocks, each containing a 1D convolutional layer, a normalization layer, a max-pooling layer, and a dropout layer. For the GR generator, we chose TimeVAE [4], where both the encoder and decoder follow a four-layer Conv1D and ConvTranspose1D structure.

Implementation Details. Following [24], all experiments were conducted five times, each with distinct class orders and random seeds. For each experimental run, hyperpa-
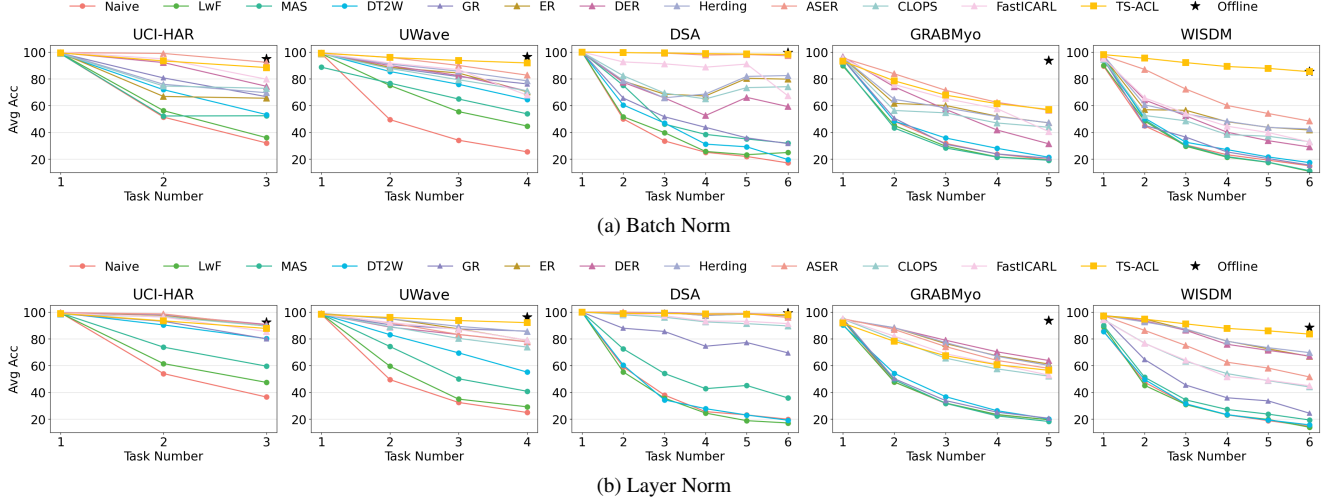
(a) Batch Norm

(b) Layer Norm

Figure 3. The accuracy of all methods on five datasets changes as the tasks progress.

Table 2. For the best-performing method in the exemplar-free approach, we use **bold** formatting, and for the best performance across all methods, we <u>underline</u> the result. The average value and standard deviation of each metric are reported based on the results of 5 runs.

(a) Batch Norm

Dataset	Metric	Naive	Offline	GR	ER	DER	Herding	ASER	CLOPS	FastICARL	LwF	MAS	DT^{2}W	TS-ACL
UCI-HAR	$\mathcal{A}_T \uparrow$	$32.00_{\pm 2.90}$	$94.94_{\pm 2.17}$	$66.66_{\pm 14.05}$	$65.46_{\pm 13.78}$	$74.41_{\pm 7.57}$	$69.58_{\pm 19.66}$	$\underline{92.36}_{\pm 2.78}$	$72.87_{\pm 11.91}$	$79.69_{\pm 7.77}$	$35.96_{\pm 11.33}$	$52.34_{\pm 15.92}$	$53.23_{\pm 16.33}$	$\mathbf{88.41}_{\pm 1.52}$
	$\mathcal{F}_T \downarrow$	$98.71_{\pm 1.38}$	N.A	$34.51_{\pm 17.06}$	$31.77_{\pm 34.66}$	$8.37_{\pm 13.59}$	$32.01_{\pm 33.80}$	$8.58_{\pm 5.00}$	$22.83_{\pm 26.62}$	$20.53_{\pm 18.20}$	$80.78_{\pm 17.46}$	$63.40_{\pm 22.78}$	$60.17_{\pm 25.07}$	$\underline{\mathbf{7.23}}_{\pm 3.08}$
UWave	$\mathcal{A}_T \uparrow$	$25.36_{\pm .59}$	$96.61_{\pm 1.05}$	$76.20_{\pm 6.25}$	$70.28_{\pm 8.21}$	$70.88_{\pm 7.71}$	$78.47_{\pm 2.87}$	$82.74_{\pm 2.01}$	$71.04_{\pm 1.66}$	$67.77_{\pm 8.62}$	$44.67_{\pm 11.64}$	$53.80_{\pm 10.36}$	$64.44_{\pm 5.92}$	$\underline{\mathbf{91.89}}_{\pm 1.72}$
	$\mathcal{F}_T \downarrow$	$91.35_{\pm 18.7}$	N.A	$27.43_{\pm 7.24}$	$36.91_{\pm 11.10}$	$35.01_{\pm 10.41}$	$26.00_{\pm 3.26}$	$21.21_{\pm 2.71}$	$35.47_{\pm 1.32}$	$39.33_{\pm 11.16}$	$51.46_{\pm 27.35}$	$40.56_{\pm 21.64}$	$32.66_{\pm 5.79}$	$\underline{\mathbf{4.05}}_{\pm 0.78}$
DSA	$\mathcal{A}_T \uparrow$	$17.04_{\pm .82}$	$99.65_{\pm .46}$	$31.51_{\pm 5.74}$	$79.75_{\pm 18.11}$	$59.19_{\pm 17.56}$	$82.42_{\pm 10.04}$	$97.26_{\pm 1.59}$	$74.10_{\pm 15.43}$	$67.28_{\pm 15.06}$	$24.82_{\pm 8.02}$	$31.82_{\pm 6.36}$	$19.56_{\pm 3.82}$	$\underline{\mathbf{98.33}}_{\pm 1.34}$
	$\mathcal{F}_T \downarrow$	$99.55_{\pm .90}$	N.A	$72.92_{\pm 9.96}$	$22.57_{\pm 19.31}$	$28.55_{\pm 30.89}$	$18.45_{\pm 12.30}$	$3.18_{\pm 1.84}$	$22.83_{\pm 22.31}$	$35.47_{\pm 19.87}$	$80.72_{\pm 13.51}$	$74.85_{\pm 13.94}$	$90.27_{\pm 10.13}$	$\underline{\mathbf{0.94}}_{\pm 1.33}$
GRABMyo	$\mathcal{A}_T \uparrow$	$19.44_{\pm .38}$	$93.63_{\pm 1.22}$	$20.59_{\pm 4.47}$	$47.03_{\pm 6.62}$	$31.38_{\pm 4.65}$	$47.14_{\pm 7.43}$	$56.50_{\pm 4.24}$	$43.75_{\pm 4.03}$	$40.55_{\pm 4.97}$	$19.22_{\pm 0.49}$	$19.04_{\pm 1.45}$	$21.34_{\pm 4.75}$	$\underline{\mathbf{57.06}}_{\pm 3.80}$
	$\mathcal{F}_T \downarrow$	$95.23_{\pm 2.43}$	N.A	$64.87_{\pm 8.64}$	$32.37_{\pm 6.28}$	$62.89_{\pm 4.34}$	$33.24_{\pm 15.75}$	$48.36_{\pm 5.16}$	$29.66_{\pm 7.33}$	$48.50_{\pm 6.76}$	$95.0_{\pm 1.5}$	$67.09_{\pm 41.90}$	$58.33_{\pm 10.10}$	$\underline{\mathbf{15.54}}_{\pm 1.42}$
WISDM	$\mathcal{A}_T \uparrow$	$14.89_{\pm 1.39}$	$85.31_{\pm 1.30}$	$42.42_{\pm 4.99}$	$48.36_{\pm 16.79}$	$32.95_{\pm 5.89}$	$32.72_{\pm 6.23}$	$14.89_{\pm 2.55}$	$10.74_{\pm 2.79}$	$17.29_{\pm 6.76}$	$15.44_{\pm 1.75}$	$41.69_{\pm 7.54}$	$28.99_{\pm 9.19}$	$\underline{\mathbf{85.35}}_{\pm 2.81}$
	$\mathcal{F}_T \downarrow$	$90.07_{\pm 8.6}$	N.A	$28.66_{\pm 11.88}$	$57.49_{\pm 19.89}$	$34.02_{\pm 13.47}$	$40.17_{\pm 9.42}$	$69.35_{\pm 34.11}$	$59.45_{\pm 18.45}$	$51.10_{\pm 30.63}$	$73.35_{\pm 10.23}$	$26.62_{\pm 12.48}$	$53.80_{\pm 28.75}$	$\underline{\mathbf{6.29}}_{\pm 0.58}$

(b) Layer Norm

Dataset	Metric	Naive	Offline	GR	ER	DER	Herding	ASER	CLOPS	FastICARL	LwF	MAS	DT^{2}W	TS-ACL
UCI-HAR	$\mathcal{A}_T \uparrow$	$36.44_{\pm 10.35}$	$92.31_{\pm .82}$	$80.04_{\pm 7.69}$	$89.53_{\pm 2.41}$	$\underline{90.75}_{\pm 1.90}$	$89.95_{\pm 2.51}$	$89.82_{\pm 1.43}$	$89.64_{\pm 1.50}$	$85.43_{\pm 3.74}$	$47.40_{\pm 14.04}$	$59.53_{\pm 15.90}$	$80.15_{\pm 6.11}$	$\mathbf{87.75}_{\pm 2.24}$
	$\mathcal{F}_T \downarrow$	$92.25_{\pm 13.25}$	N.A	$25.75_{\pm 15.74}$	$9.53_{\pm 6.54}$	$8.58_{\pm 5.97}$	$9.96_{\pm 7.24}$	$10.20_{\pm 5.57}$	$8.98_{\pm 4.82}$	$17.51_{\pm 8.25}$	$74.04_{\pm 22.17}$	$52.47_{\pm 27.00}$	$16.55_{\pm 9.33}$	$\underline{\mathbf{6.29}}_{\pm 2.87}$
UWave	$\mathcal{A}_T \uparrow$	$24.85_{\pm 0.12}$	$96.39_{\pm 0.22}$	$85.77_{\pm 3.76}$	$78.89_{\pm 4.27}$	$77.74_{\pm 6.51}$	$85.42_{\pm 1.89}$	$77.89_{\pm 5.26}$	$73.79_{\pm 3.39}$	$79.01_{\pm 0.98}$	$29.09_{\pm 5.34}$	$40.74_{\pm 9.29}$	$55.09_{\pm 9.27}$	$\underline{\mathbf{92.12}}_{\pm 1.75}$
	$\mathcal{F}_T \downarrow$	$98.15_{\pm 1.4}$	N.A	$15.37_{\pm 4.48}$	$25.87_{\pm 5.68}$	$27.31_{\pm 7.67}$	$16.51_{\pm 1.82}$	$27.14_{\pm 6.33}$	$32.12_{\pm 2.95}$	$25.60_{\pm 2.24}$	$73.47_{\pm 25.06}$	$65.01_{\pm 15.14}$	$40.28_{\pm 16.04}$	$\underline{\mathbf{3.72}}_{\pm 1.31}$
DSA	$\mathcal{A}_T \uparrow$	$19.81_{\pm 4.12}$	$99.53_{\pm 0.76}$	$69.50_{\pm 7.26}$	$97.24_{\pm 1.43}$	$\underline{98.01}_{\pm 0.69}$	$97.75_{\pm 1.36}$	$95.97_{\pm 6.32}$	$89.65_{\pm 5.51}$	$91.39_{\pm 6.16}$	$17.01_{\pm 4.33}$	$35.75_{\pm 6.35}$	$19.06_{\pm 4.11}$	$\mathbf{98.12}_{\pm 1.75}$
	$\mathcal{F}_T \downarrow$	$96.23_{\pm 4.95}$	N.A	$36.43_{\pm 8.64}$	$3.25_{\pm 1.78}$	$2.28_{\pm 0.82}$	$2.62_{\pm 1.59}$	$4.73_{\pm 7.55}$	$12.30_{\pm 6.64}$	$10.28_{\pm 7.44}$	$87.93_{\pm 15.21}$	$66.17_{\pm 14.57}$	$96.85_{\pm 4.81}$	$\underline{\mathbf{0.98}}_{\pm 1.08}$
GRABMyo	$\mathcal{A}_T \uparrow$	$19.46_{\pm .34}$	$93.83_{\pm 0.87}$	$20.56_{\pm 1.37}$	$\underline{61.16}_{\pm 3.30}$	$63.78_{\pm 3.96}$	$60.07_{\pm 3.69}$	$57.90_{\pm 4.79}$	$52.05_{\pm 5.11}$	$52.84_{\pm 3.49}$	$19.42_{\pm 0.32}$	$18.15_{\pm 1.57}$	$20.09_{\pm 7.28}$	$\mathbf{56.44}_{\pm 3.22}$
	$\mathcal{F}_T \downarrow$	$94.17_{\pm 3.34}$	N.A	$94.44_{\pm 3.13}$	$40.87_{\pm 3.59}$	$37.01_{\pm 3.68}$	$42.46_{\pm 4.02}$	$45.49_{\pm 5.48}$	$52.22_{\pm 5.54}$	$52.46_{\pm 4.19}$	$93.25_{\pm 6.64}$	$88.34_{\pm 7.52}$	$22.57_{\pm 9.52}$	$\underline{\mathbf{15.75}}_{\pm 1.69}$
WISDM	$\mathcal{A}_T \uparrow$	$14.60_{\pm 2.25}$	$88.60_{\pm 1.94}$	$24.33_{\pm 8.12}$	$66.88_{\pm 7.36}$	$67.14_{\pm 5.37}$	$69.67_{\pm 3.98}$	$51.48_{\pm 15.85}$	$44.00_{\pm 8.11}$	$44.87_{\pm 3.67}$	$13.83_{\pm 3.51}$	$19.25_{\pm 6.66}$	$15.59_{\pm 7.92}$	$\underline{\mathbf{83.53}}_{\pm 2.87}$
	$\mathcal{F}_T \downarrow$	$88.47_{\pm 10.58}$	N.A	$85.78_{\pm 10.00}$	$33.80_{\pm 7.90}$	$33.38_{\pm 6.67}$	$30.04_{\pm 3.98}$	$53.04_{\pm 18.68}$	$60.74_{\pm 10.12}$	$52.79_{\pm 6.37}$	$83.53_{\pm 17.51}$	$74.65_{\pm 12.06}$	$37.50_{\pm 14.48}$	$\underline{\mathbf{7.13}}_{\pm 1.69}$

rameter tuning was performed through two validation iterations on validation tasks. All models were trained using the Adam optimizer with a learning rate of 0.001 and a batch size of 64, with 100 epochs for the first task and subsequent tasks and the learning rate scheduler is treated as a hyperparameter and is tuned during the validation tasks. However, TS-ACL diverges from this by bypassing gradient descent after the initial task, opting instead for an analytical update method that requires only a single epoch. During incremental learning, TS-ACL employs a frozen en-

coder with an appended RHL. Data preprocessing includes a non-trainable input normalization layer applied before the encoder to standardize inputs on a per-sample basis. Specific normalization methods were used for each dataset: layer normalization for UCI-HAR, DSA, and GRABMyo; instance normalization for UWave; and no normalization for WISDM. The encoder's architecture integrates two normalization types: Batch Normalization (BN) and Layer Normalization (LN). For replay-based methods, we set the memory storage pool to 5%. For TS-ACL, we configure γ
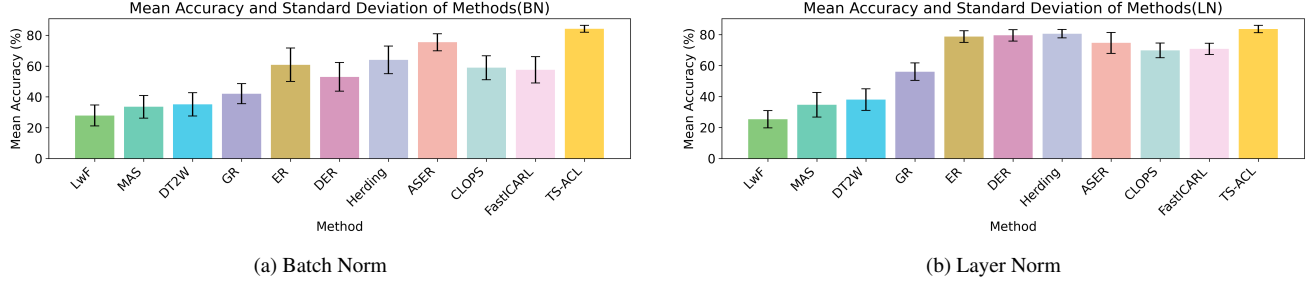
(a) Batch Norm

(b) Layer Norm

Figure 4. The performance of each method is averaged across the five datasets.
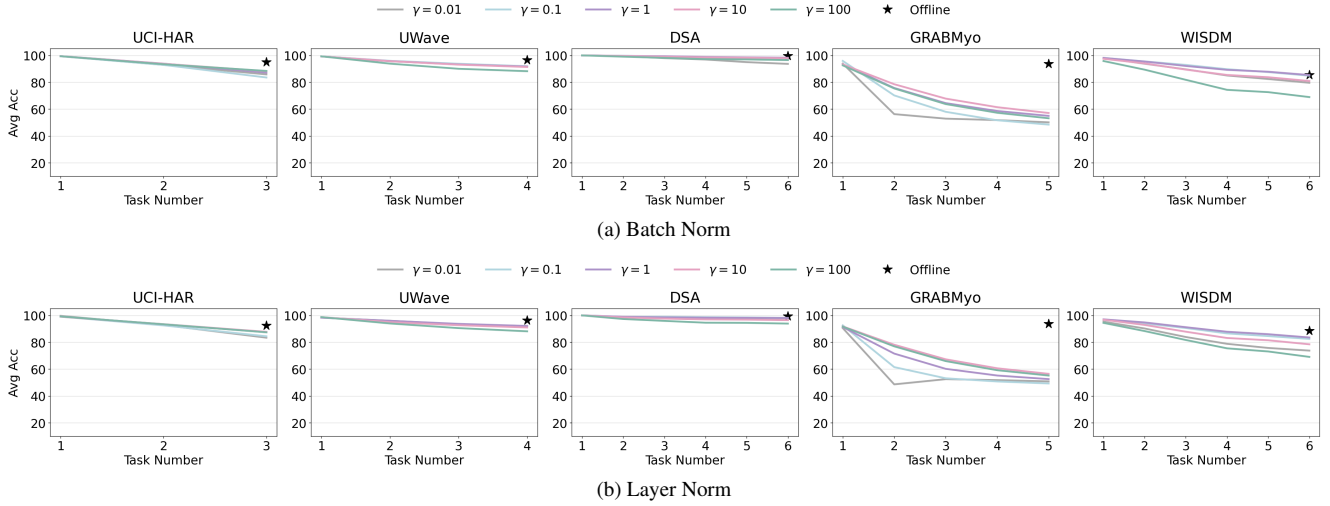

(a) Batch Norm

(b) Layer Norm

Figure 5. The accuracy of TS-ACL on five datasets varies with different γ values as tasks progress.

to {0.01, 0.1, 1, 10, 100} and set the embedding expansion size to 8192. We select the best γ value to present in the experimental results. See supplementary for more details.

4.2. Main Results

Plasticity. As demonstrated in Table 2 and Figure 3, TS-ACL achieves remarkable accuracy across five datasets. Under the exemplar-free approach, TS-ACL consistently outperforms the best existing methods. In the BN setting, TS-ACL surpasses the second-best method by 35.18%, 27.45%, 66.51%, 35.72%, and 43.66% across the five datasets. In the LN setting, TS-ACL surpasses the second-best method by 7.6%, 37.03%, 62.37%, 36.41%, and 64.28%, respectively. In fact, on most datasets, TS-ACL outperforms all methods, including the second-best by 9.15%, 1.07%, 0.56%, and 37.00% in the BN setting for UWave, DSA, GRABMyo, and WSIDM, respectively, and by 6.70%, 0.11%, 13.86% in the LN setting for UWave, DSA, and WSIDM, respectively. These results underscore TS-ACL's superior performance in terms of plasticity.

Stability. As shown in Table 2, our TS-ACL achieves the lowest forgetting rate across all datasets, under both

BN and LN conditions. Specifically, under BN, it surpasses the strongest baseline model by 1.35%, 17.16%, 2.24%, 16.83%, and 20.33% on the five datasets, respectively. Likewise, under LN, it outperforms the strongest baseline by 2.29%, 12.79%, 1.3%, 6.82%, and 22.91%, respectively. This superior performance can be attributed to the fact that TS-ACL is mathematically proven to achieve results comparable to joint learning in the context of incremental learning, which has the remarkable property of **non-forgetting**, as discussed in Section 3.4.

4.3. Robustness Analyses

Class Order Robustness. For each dataset and method, we conducted experiments five times, each with a different random seed, resulting in varying class orders across each run. We then averaged the final task accuracy and standard deviation of each method across five datasets, as illustrated in Figure 4 according to Table 2. The results indicate that the TS-ACL achieves the highest average accuracy and the lowest standard deviation, Here, we primarily focus on the magnitude of the standard deviation, as it directly reflects the robustness of each method under different Class Order

Table 3. $\mathcal{A}_T$ and $\mathcal{F}_T$ on all benchmark datasets with various values of the regularization term γ.

(a) Batch Norm

γ	UCI-HAR (%)		UWave (%)		DSA (%)		GRABMyo (%)		WISDM (%)	
	$\mathcal{A}_T \uparrow$	$\mathcal{F}_T \downarrow$	$\mathcal{A}_T \uparrow$	$\mathcal{F}_T \downarrow$	$\mathcal{A}_T \uparrow$	$\mathcal{F}_T \downarrow$	$\mathcal{A}_T \uparrow$	$\mathcal{F}_T \downarrow$	$\mathcal{A}_T \uparrow$	$\mathcal{F}_T \downarrow$
0.01	85.83 ± 2.71	9.57 ± 2.09	91.67 ± 1.66	4.11 ± 1.11	93.67 ± 8.37	4.37 ± 8.92	50.11 ± 4.02	$\mathbf{10.45 \pm 1.97}$	79.57 ± 9.63	10.24 ± 7.44
0.1	83.53 ± 1.64	10.16 ± 3.34	$\mathbf{91.89 \pm 1.72}$	4.05 ± 0.78	96.50 ± 5.61	2.75 ± 5.66	48.43 ± 2.93	15.76 ± 2.04	84.86 ± 2.11	6.82 ± 1.51
1	87.15 ± 1.37	7.70 ± 3.32	91.68 ± 2.24	$\mathbf{3.96 \pm 1.34}$	98.26 ± 2.25	$\mathbf{1.33 \pm 2.33}$	54.91 ± 3.37	15.43 ± 2.32	$\mathbf{85.35 \pm 2.81}$	$\mathbf{6.29 \pm 0.58}$
10	88.20 ± 1.40	7.29 ± 3.03	91.35 ± 2.10	3.98 ± 1.26	97.89 ± 1.47	1.38 ± 1.38	$\mathbf{57.06 \pm 3.80}$	15.54 ± 1.42	80.89 ± 3.39	8.45 ± 0.92
100	$\mathbf{88.41 \pm 1.52}$	$\mathbf{7.23 \pm 3.08}$	88.21 ± 2.61	4.45 ± 1.18	96.54 ± 1.57	2.28 ± 1.64	53.14 ± 4.96	15.70 ± 1.67	68.92 ± 6.53	12.81 ± 2.40

(b) Layer Norm

γ	UCI-HAR (%)		UWave (%)		DSA (%)		GRABMyo (%)		WISDM (%)	
	$\mathcal{A}_T \uparrow$	$\mathcal{F}_T \downarrow$	$\mathcal{A}_T \uparrow$	$\mathcal{F}_T \downarrow$	$\mathcal{A}_T \uparrow$	$\mathcal{F}_T \downarrow$	$\mathcal{A}_T \uparrow$	$\mathcal{F}_T \downarrow$	$\mathcal{A}_T \uparrow$	$\mathcal{F}_T \downarrow$
0.01	83.38 ± 1.42	9.50 ± 3.06	92.05 ± 0.72	$\mathbf{3.45 \pm 0.94}$	96.49 ± 2.47	1.88 ± 1.85	50.82 ± 3.45	$\mathbf{9.44 \pm 2.33}$	73.75 ± 6.85	12.05 ± 6.86
0.1	84.43 ± 2.77	8.33 ± 2.80	91.80 ± 1.02	3.89 ± 1.75	$\mathbf{98.12 \pm 1.07}$	$\mathbf{0.98 \pm 1.08}$	49.27 ± 5.34	12.24 ± 3.37	82.46 ± 4.76	8.22 ± 4.17
1	87.47 ± 2.56	7.03 ± 3.39	$\mathbf{92.12 \pm 1.75}$	3.72 ± 1.31	98.03 ± 1.14	1.02 ± 1.16	52.52 ± 3.37	14.79 ± 2.48	$\mathbf{83.53 \pm 2.87}$	$\mathbf{7.13 \pm 1.69}$
10	$\mathbf{87.75 \pm 2.24}$	$\mathbf{6.29 \pm 2.87}$	91.00 ± 2.52	4.31 ± 1.78	96.44 ± 1.82	1.90 ± 1.48	$\mathbf{56.44 \pm 3.22}$	15.54 ± 1.42	78.45 ± 4.16	9.17 ± 1.58
100	87.38 ± 2.08	7.12 ± 3.63	88.12 ± 2.65	4.88 ± 1.37	93.89 ± 1.81	3.18 ± 1.62	55.17 ± 2.73	15.55 ± 1.32	69.06 ± 5.28	12.23 ± 1.39

settings. Among all the comparison methods, our approach maintains the smallest standard deviation, indicating that our method exhibits the strongest class order robustness.

Why TS-ACL has class order robustness? As demonstrated in 3.4, the effectiveness of our TS-ACL in incremental continual learning is equivalent to that of joint learning. This ***weight-invariant*** property ensures that our method achieves nearly consistent performance across different class order settings, with only minor standard deviation due to the slight differences in encoding parameters learned during the first task. This property guarantees robust performance across various class order settings.

Norm Robustness. As shown in Figure 3 and Table 2, for TS-ACL, the performance difference between BN and LN is negligible. In replay-based methods, due to BN's reliance on batch statistics, is particularly vulnerable to the impact of imbalanced distributions between new and old samples in incremental learning. This imbalance not only contributes to the forgetting of previously learned knowledge but also hinders the acquisition of new information [21]. In contrast, LN through instance normalization, effectively alleviates these issues, demonstrating superior performance. However, ASER exhibits a little performance gap between BN and LN, as hypothesized in [24]. ASER selects a balanced and representative set of memory samples, which helps maintain unbiased statistics under BN.

Why TS-ACL has norm robustness? Our TS-ACL possesses norm robustness because it is trained using analytical learning, with the encoder functioning as a frozen embedding extractor that does not require gradient updates or backpropagation during continual learning. Therefore, BN and LN fundamentally only modify embedding extraction, and the extracted embeddings can be considered to contain similar representations. As a result, they do not significantly impact the classification. In comparison to exemplar-free methods, the effectiveness of BN or LN depends on the specific approach used. The attribute of norm robustness within our TS-ACL provides a unique advantage, as it has minimal impact on results, allowing us to avoid repeated experiments to find the optimal normalization way.

Regularization Term Analysis. As shown in Figure 5 and Table 3, overall, γ is relatively stable across a broad range of values (e.g. $\{0.01, 0.1, 1, 10, 100\}$). However, on the second task of the GRABMyo dataset, a significant performance drop is observed when γ is set to 0.01 and 0.1, which is due to overfitting. Additionally, on the Wisdom dataset, when γ is set to 100, performance declines notably due to underfitting, as the simplicity of the linear regression becomes apparent [37].

5. Conclusion

In this study, we propose TS-ACL, an analytical continual learning framework for time series class-incremental pattern recognition that fundamentally addresses the problem of catastrophic forgetting through gradient-free recursive regression learning, while also achieving privacy preservation and efficiency. Experimental results demonstrate that TS-ACL significantly outperforms existing methods across five benchmark datasets, achieving both stability and plasticity, and simultaneously possessing the non-forgetting property and weight-invariant property, making it a robust solution, particularly in resource-constrained scenarios such as edge computing.

References

[1] Rahaf Aljundi, Francesca Babiloni, Mohamed Elhoseiny, Marcus Rohrbach, and Tinne Tuytelaars. Memory aware synapses: Learning what (not) to forget. In *Proceedings of the European conference on computer vision (ECCV)*, pages 139–154, 2018. 2, 5

[2] Kerem Altun and Billur Barshan. Human activity recognition using inertial/magnetic sensor units. In *Human Behavior Understanding: First International Workshop, HBU 2010, Istanbul, Turkey, August 22, 2010. Proceedings 1*, pages 38–51. Springer, 2010. 5

[3] Pietro Buzzega, Matteo Boschini, Angelo Porrello, Davide Abati, and Simone Calderara. Dark experience for general continual learning: a strong, simple baseline. *Advances in neural information processing systems*, 33:15920–15930, 2020. 5

[4] Abhyuday Desai, Cynthia Freeman, Zuhui Wang, and Ian Beaver. Timevae: A variational auto-encoder for multivariate time series generation. *arXiv preprint arXiv:2111.08095*, 2021. 5

[5] Ian J Goodfellow, Mehdi Mirza, Da Xiao, Aaron Courville, and Yoshua Bengio. An empirical investigation of catastrophic forgetting in gradient-based neural networks. *arXiv preprint arXiv:1312.6211*, 2013. 1, 2, 3

[6] Ping Guo, Michael R Lyu, and NE Mastorakis. Pseudoinverse learning algorithm for feedforward neural networks. *Advances in Neural Networks and Applications*, 1(321-326), 2001. 3

[7] Dewi Pramudi Ismi, Shireen Panchoo, and Murinto Murinto. K-means clustering based filter feature selection on high dimensional data. *International Journal of Advances in Intelligent Informatics*, 2(1):38–45, 2016. 5

[8] Ming Jin, Huan Yee Koh, Qingsong Wen, Daniele Zambon, Cesare Alippi, Geoffrey I. Webb, Irwin King, and Shirui Pan. A survey on graph neural networks for time series: Forecasting, classification, imputation, and anomaly detection. *IEEE Transactions on Pattern Analysis and Machine Intelligence*, 2024. 2

[9] Rohit J Kate. Using dynamic time warping distances as features for improved time series classification. *Data mining and knowledge discovery*, 30:283–312, 2016. 2

[10] Dani Kiyasseh, Tingting Zhu, and David Clifton. A clinical deep learning framework for continually learning from cardiac signals across diseases, time, modalities, and institutions. *Nature Communications*, 12(1):4221, 2021. 1, 5

[11] Young D Kwon, Jagmohan Chauhan, and Cecilia Mascolo. Fasticarl: Fast incremental classifier and representation learning with efficient budget allocation in audio sensing applications. *arXiv preprint arXiv:2106.07268*, 2021. 2, 5

[12] Zhizhong Li and Derek Hoiem. Learning without forgetting. *IEEE transactions on pattern analysis and machine intelligence*, 40(12):2935–2947, 2017. 2, 5

[13] Yuxuan Liang, Haomin Wen, Yuqi Nie, Yushan Jiang, Ming Jin, Dongjin Song, Shirui Pan, and Qingsong Wen. Foundation models for time series analysis: A tutorial and survey. In *Proceedings of the 30th ACM SIGKDD Conference on Knowledge Discovery and Data Mining*, pages 6555–6565, 2024. 1

[14] Jason Lines and Anthony Bagnall. Time series classification with ensembles of elastic distance measures. *Data Mining and Knowledge Discovery*, 29:565–592, 2015. 2

[15] Jason Lines, Sarah Taylor, and Anthony Bagnall. Time series classification with hive-cote: The hierarchical vote collective of transformation-based ensembles. *ACM Transactions on Knowledge Discovery from Data (TKDD)*, 12(5):1–35, 2018. 2

[16] Jiayang Liu, Lin Zhong, Jehan Wickramasuriya, and Venu Vasudevan. uwave: Accelerometer-based personalized gesture recognition and its applications. *Pervasive and Mobile Computing*, 5(6):657–675, 2009. 5

[17] Siliang Lu, Jingfeng Lu, Kang An, Xiaoxian Wang, and Qingbo He. Edge computing on iot for machine signal processing and fault diagnosis: A review. *IEEE Internet of Things Journal*, 10(13):11093–11116, 2023. 2, 3

[18] Matthew Middlehurst, James Large, Michael Flynn, Jason Lines, Aaron Bostrom, and Anthony Bagnall. Hive-cote 2.0: a new meta ensemble for time series classification. *Machine Learning*, 110(11):3211–3243, 2021. 2

[19] Navid Mohammadi Foumani, Lynn Miller, Chang Wei Tan, Geoffrey I. Webb, Germain Forestier, and Mahsa Salehi. Deep learning for time series classification and extrinsic regression: A current survey. *ACM Comput. Surv.*, 56(9), 2024. 2

[20] Jooyoung Park and Irwin W Sandberg. Universal approximation using radial-basis-function networks. *Neural computation*, 3(2):246–257, 1991. 3

[21] Quang Pham, Chenghao Liu, and Steven Hoi. Continual normalization: Rethinking batch normalization for online continual learning. *arXiv preprint arXiv:2203.16102*, 2022. 8

[22] Ashirbad Pradhan, Jiayuan He, and Ning Jiang. Multi-day dataset of forearm and wrist electromyogram for hand gesture recognition and biometrics. *Scientific data*, 9(1):733, 2022. 5

[23] Zhongzheng Qiao, Minghui Hu, Xudong Jiang, Ponnuthurai Nagaratnam Suganthan, and Ramasamy Savitha. Class-incremental learning on multivariate time series via shape-aligned temporal distillation. In *ICASSP 2023-2023 IEEE International Conference on Acoustics, Speech and Signal Processing (ICASSP)*, pages 1–5. IEEE, 2023. 1, 2, 5

[24] Zhongzheng Qiao, Quang Pham, Zhen Cao, Hoang H Le, Ponnuthurai N Suganthan, Xudong Jiang, and Ramasamy Savitha. Class-incremental learning for time series: Benchmark and evaluation. *arXiv preprint arXiv:2402.12035*, 2024. 4, 5, 8

[25] Sylvestre-Alvise Rebuffi, Alexander Kolesnikov, Georg Sperl, and Christoph H Lampert. icarl: Incremental classifier and representation learning. In *Proceedings of the IEEE conference on Computer Vision and Pattern Recognition*, pages 2001–2010, 2017. 2, 5

[26] David Rolnick, Arun Ahuja, Jonathan Schwarz, Timothy Lillicrap, and Gregory Wayne. Experience replay for continual learning. *Advances in neural information processing systems*, 32, 2019. 2, 5

[27] Dongsub Shim, Zheda Mai, Jihwan Jeong, Scott Sanner, Hyunwoo Kim, and Jongseong Jang. Online class-incremental continual learning with adversarial shapley value. In *Proceedings of the AAAI Conference on Artificial Intelligence*, pages 9630–9638, 2021. 5

[28] Hanul Shin, Jung Kwon Lee, Jaehong Kim, and Jiwon Kim. Continual learning with deep generative replay. *Advances in neural information processing systems*, 30, 2017. 2, 5

[29] Chang Wei Tan, François Petitjean, and Geoffrey I Webb. Fastee: fast ensembles of elastic distances for time series classification. *Data Mining and Knowledge Discovery*, 34 (1):231–272, 2020. 2

[30] Jonathan Tapson and André van Schaik. Learning the pseudoinverse solution to network weights. *Neural Networks*, 45: 94–100, 2013. 3

[31] Jingyuan Wang, Chen Yang, Xiaohan Jiang, and Junjie Wu. When: A wavelet-dtw hybrid attention network for heterogeneous time series analysis. In *Proceedings of the 29th ACM SIGKDD Conference on Knowledge Discovery and Data Mining*, pages 2361–2373, 2023. 2

[32] Lin Wang, Zheng Yin, Mamta Puppala, Chika F. Ezeana, Kelvin K. Wong, Tiancheng He, Deepa B. Gotur, and Stephen T. C. Wong. A time-series feature-based recursive classification model to optimize treatment strategies for improving outcomes and resource allocations of covid-19 patients. *IEEE Journal of Biomedical and Health Informatics*, 26(7):3323–3329, 2022. 1, 2

[33] Liyuan Wang, Xingxing Zhang, Hang Su, and Jun Zhu. A comprehensive survey of continual learning: Theory, method and application. *IEEE Transactions on Pattern Analysis and Machine Intelligence*, 46(8):5362–5383, 2024. 1, 2, 3, 4

[34] Xi-Zhao Wang, Tianlun Zhang, and Ran Wang. Noniterative deep learning: Incorporating restricted boltzmann machine into multilayer random weight neural networks. *IEEE Transactions on Systems, Man, and Cybernetics: Systems*, 49(7): 1299–1308, 2019. 3

[35] Gary M Weiss. Wisdm smartphone and smartwatch activity and biometrics dataset. *UCI Machine Learning Repository: WISDM Smartphone and Smartwatch Activity and Biometrics Dataset Data Set*, 7:133190–133202, 2019. 5

[36] Wenbiao Yang, Kewen Xia, Zhaocheng Wang, Shurui Fan, and Ling Li. Self-attention causal dilated convolutional neural network for multivariate time series classification and its application. *Engineering Applications of Artificial Intelligence*, 122:106151, 2023. 1, 2

[37] Huiping Zhuang, Zhiping Lin, and Kar-Ann Toh. Correlation projection for analytic learning of a classification network. *Neural Processing Letters*, 53:3893–3914, 2021. 8

[38] Huiping Zhuang, Zhenyu Weng, Hongxin Wei, Renchunzi Xie, Kar-Ann Toh, and Zhiping Lin. ACIL: Analytic class-incremental learning with absolute memorization and privacy protection. In *Advances in Neural Information Processing Systems*, pages 11602–11614. Curran Associates, Inc., 2022. 3

[39] Huiping Zhuang, Zhenyu Weng, Run He, Zhiping Lin, and Ziqian Zeng. Gkeal: Gaussian kernel embedded analytic learning for few-shot class incremental task. In *Proceedings of the IEEE/CVF conference on computer vision and pattern recognition*, pages 7746–7755, 2023. 2, 3

[40] Huiping Zhuang, Run He, Kai Tong, Ziqian Zeng, Cen Chen, and Zhiping Lin. DS-AL: A dual-stream analytic learning for exemplar-free class-incremental learning. In *Proceedings of the AAAI Conference on Artificial Intelligence*, pages 17237–17244, 2024. 2, 3

TS-ACL: A Time Series Analytic Continual Learning Framework for Privacy-Preserving and Class-Incremental Pattern Recognition

Supplementary Material

A. Proof of Theorem

In this section, we provide a mathematical proof for Theorem 1.

We prove Theorem 1 using the solution of joint training on t tasks with ridge regression:

$$\hat{\boldsymbol{\Phi}}_t = \left(\mathbf{U}_{1:t}^{(E)\top} \mathbf{U}_{1:t}^{(E)} + \gamma \mathbf{I} \right)^{-1} \mathbf{U}_{1:t}^{(E)\top} \mathbf{V}_{1:t}. \tag{13}$$

By decoupling the t-th task from previous tasks, $\hat{\boldsymbol{\Phi}}_t$ can be written as:

$$\hat{\boldsymbol{\Phi}}_t = \left(\begin{bmatrix} \mathbf{U}_{1:t-1}^{(E)\top} & \mathbf{U}_t^{(E)\top} \end{bmatrix} \begin{bmatrix} \left(\mathbf{U}_{1:t-1}^{(E)} \right) \\ \left(\mathbf{U}_t^{(E)} \right) \end{bmatrix} + \gamma \mathbf{I} \right)^{-1} \begin{bmatrix} \mathbf{U}_{1:t-1}^{(E)\top} & \mathbf{U}_t^{(E)\top} \end{bmatrix} \begin{bmatrix} \mathbf{V}_{1:t-1} & \mathbf{0} \\ \mathbf{0} & \mathbf{V}_t^{\text{train}} \end{bmatrix}$$

$$= \left(\mathbf{U}_{1:t-1}^{(E)\top} \mathbf{U}_{1:t-1}^{(E)} + \gamma \mathbf{I} + \mathbf{U}_t^{(E)\top} \mathbf{U}_t^{(E)} \right)^{-1} \begin{bmatrix} \mathbf{U}_{1:t-1}^{(E)\top} \mathbf{V}_{1:t-1} & \mathbf{U}_t^{(E)\top} \mathbf{V}_t^{\text{train}} \end{bmatrix}. \tag{14}$$

We introduce the memory matrix as in the following definition:

$$\boldsymbol{\Psi}_t = \left(\mathbf{U}_{1:t}^{(E)\top} \mathbf{U}_{1:t}^{(E)} + \gamma \mathbf{I} \right)^{-1}, \tag{15}$$

which is the matrix inversion term of Eqn 13.

Noticing that $\boldsymbol{\Psi}_{t-1} = \left(\mathbf{U}_{1:t-1}^{(E)\top} \mathbf{U}_{1:t-1}^{(E)} + \gamma \mathbf{I} \right)^{-1}$, by Woodbury matrix identity where $(\mathbf{A} + \mathbf{U}\mathbf{C}\mathbf{V})^{-1} = \mathbf{A}^{-1} - \mathbf{A}^{-1}\mathbf{U} \left(\mathbf{C}^{-1} + \mathbf{V}\mathbf{A}^{-1}\mathbf{U} \right)^{-1} \mathbf{V}\mathbf{A}^{-1}$ and treating $\boldsymbol{\Psi}_{t-1}$ as $\mathbf{A}^{-1}$, the memory at the t-th step can be further defined as a recursive solution:

$$\boldsymbol{\Psi}_t = \boldsymbol{\Psi}_{t-1} - \boldsymbol{\Psi}_{t-1} \mathbf{U}_t^{(E)\top} \left(\mathbf{I} + \mathbf{U}_t^{(E)} \boldsymbol{\Psi}_{t-1} \mathbf{U}_t^{(E)\top} \right)^{-1} \mathbf{U}_t^{(E)} \boldsymbol{\Psi}_{t-1}. \tag{16}$$

Thus, the parameter $\hat{\boldsymbol{\Phi}}_t$ is derived as

$$\hat{\boldsymbol{\Phi}}_t = \begin{bmatrix} \boldsymbol{\Psi}_t \mathbf{U}_{1:t-1}^{(E)\top} \mathbf{V}_{1:t-1} & \boldsymbol{\Psi}_t \mathbf{U}_t^{(E)\top} \mathbf{V}_t^{\text{train}} \end{bmatrix}. \tag{17}$$

Denote the left submatrix $\boldsymbol{\Psi}_t \mathbf{U}_{1:t-1}^{(E)\top} \mathbf{V}_{1:t-1}$ as $\mathbf{H}$. By substituting Eqn 16 into 17,

$$\mathbf{H} = \hat{\boldsymbol{\Phi}}_{t-1} - \boldsymbol{\Psi}_{t-1} \mathbf{U}_t^{(E)\top} \left(\mathbf{I} + \mathbf{U}_t^{(E)} \boldsymbol{\Psi}_{t-1} \mathbf{U}_t^{(E)\top} \right)^{-1} \mathbf{U}_t^{(E)} \hat{\boldsymbol{\Phi}}_{t-1}. \tag{18}$$

Based on the identity $(\mathbf{I} + \mathbf{P})^{-1} = \mathbf{I} - (\mathbf{I} + \mathbf{P})^{-1} \mathbf{P}$, it is further derived as:

$$\mathbf{H} = \hat{\boldsymbol{\Phi}}_{t-1} - \boldsymbol{\Psi}_t \mathbf{U}_t^{(E)\top} \mathbf{U}_t^{(E)} \hat{\boldsymbol{\Phi}}_{t-1}. \tag{19}$$

Thus,

$$\hat{\boldsymbol{\Phi}}_t = \begin{bmatrix} \hat{\boldsymbol{\Phi}}_{t-1} - \boldsymbol{\Psi}_t \mathbf{U}_t^{(E)\top} \mathbf{U}_t^{(E)} \hat{\boldsymbol{\Phi}}_{t-1} & \boldsymbol{\Psi}_t \mathbf{U}_t^{(E)\top} \mathbf{V}_t^{\text{train}} \end{bmatrix}. \tag{20}$$

Theorem 1 is thus proved.

B. More Implementation Details

The learning rate scheduler was optimized as a hyperparameter, alongside the use of early stopping to mitigate overfitting and patience values were set at 20 for ER- and GR-based methods and at 5 for other approaches. To facilitate early stopping, a validation set was created by dividing the training data in a 1:9 ratio, with validation loss monitored. Three learning rate scheduling strategies were evaluated: Step10, Step15, and OneCycleLR. In Step10 and Step15, the learning rate decreased by a factor of 0.1 at the 10th and 15th epochs, respectively. Dropout rates varied across datasets: 0 for UCI-HAR and UWave, and 0.3 for DSA, GRABMyo, and WISDM. For additional information, please refer to our code.

C. Dataset Details

UCI-HAR dataset includes temporal sequences obtained from smartphone inertial sensors during the execution of six daily activities. Data were collected at a frequency of 50Hz from 30 participants of varying ages. Each input sequence consists of nine channels, covering a temporal span of 128 timesteps.

UWave provides over 4000 samples collected from eight individuals performing eight distinct gesture patterns. The data consists of time series captured along three accelerometer axes, with each sample having a dimensionality of 3 and spanning 315 timesteps.

DSA gathers motion sensor data from 19 different sports activities performed by eight volunteers. Each segment serves as a single sample, featuring data across 45 channels and 125 timesteps. For uniformity among classes, 18 activity classes were selected for experimentation.

GRABMyo is a comprehensive surface electromyography (sEMG) dataset designed for hand gesture recognition. It includes signals corresponding to 16 gestures performed by 43 participants across three sessions. Recordings last five seconds, sampled from 28 channels at 2048 Hz. For experimentation, data from a single session were used and downsampled to 256 Hz. A non-overlapping sliding window of 0.5 seconds (128 timesteps) was applied to segment the signals into samples. The data were then split into training and testing sets in a 3:1 ratio, ensuring both sets include all subjects to mitigate distribution shifts across participants.

WISDM is a human activity recognition dataset that captures sensor data from 18 activities performed by 51 participants. Using the phone accelerometer modality, samples were generated with a non-overlapping sliding window of 200, representing 10-second time series collected at a 20Hz frequency. Like GRABMyo, the data were split into training and test sets at a 3:1 ratio, ensuring all participants are represented in both splits.

D. Algorithm

Algorithm 1 The Proposed TS-ACL Framework

Require: Total number of tasks T; Training time series datasets $\{\mathcal{D}_t^{\text{train}}\}_{t=1}^T$; Regularization parameter γ; embedding expansion size d_{E}

Ensure: Final model parameters Θ_{encoder} and $\hat{\mathbf{\Phi}}_T$

1: **Gradient Descent-Based Training**
2: Train the network on $\mathcal{D}_1^{\text{train}}$ using gradient descent
3: Save and freeze the encoder weights Θ_{encoder}

4: **Regression-Based Coordinate**
5: Extract and expand embeddings using Eq.(2), Eq.(3)
6: Compute initial classifier weights using Eq.(5)
7: Compute aggregated temporal inverse correlation matrix using Eq.(10)

8: **Recursive Regression-Based Learning**
9: **for** $t = 2$ to T **do**
10:    Extract and expand embeddings using Eq.(2), Eq.(3)
11:    Update aggregated temporal inverse correlation matrix using Eq.(12)
12:    Update classifier weights using Eq.(11)
13: **end for**

14: **Output**: Final model parameters Θ_{encoder} and $\hat{\mathbf{\Phi}}_T$